Non-dispersive and Air-stable Electron Transport in an Amorphous Organic Semiconductor

H. Murata,[a*] G. G. Malliaras,[b] M. Uchida,[c] Y. Shen, [b] and Z. H. Kafafi [a **]

[a] Optical Sciences Division, US Naval Research Laboratory, Washington, DC 20375, USA.

[b] Department of Materials Science and Engineering, Cornell University, Ithaca, NY 14853, USA.

[c] Chisso Corporation, 5-1 Ookawa Kanazawa, Yokohama, Kanagawa 236-8605, Japan.

Abstract

We report the electron transport properties of an amorphous organic semiconductor based on silole derivatives. The observed non-dispersive and fast electron transport suggests that electron trapping due to energetic disorder is very small. Based on the mobility measurements in air we conclude that oxygen does not function as a significant electron trap. The observed excellent electron transport properties of this silole derivative are attributed to a large electron affinity originating from its σ^*-π^* conjugation and a high aromaticity of its anionic species.

* Corresponding author. Fax +1-202-404-8114; e-mail: murata@ccs.nrl.navy.mil
** E-Mail: Kafafi@ccf.nrl.navy.mil

1. Introduction

Electron-transporting organic semiconductors (ETOS) are an important class of materials. They play crucial roles in electronic and optoelectronic devices such as organic light-emitting diodes (OLEDs), bipolar transistors and photovoltaic cells, and have a strong influence on their power consumption, efficiency and overall performance. Most of the organic semiconductors developed to date are hole conductors. In particular, very few organic compounds have substantially high electron mobilities, especially in air.

There are two primary approaches for achieving high electron mobilities. One is to improve morphological order in organic solid films. By changing film morphology from amorphous, polycrystalline to single crystal, both hole and electron mobilities are drastically increased. For example, precisely prepared pentacene single crystals show very high electron mobility (1.7 cm^2/Vs) at room temperature, but imperfect purification and uncontrolled crystallization readily decreases the mobility by at least three orders of magnitude. (*1*) Among organic materials, C_{60} single crystals show the highest electron mobility (2.1 cm^2/Vs). (*2*) However, C_{60} crystals cannot maintain such excellent mobility in air due to the strong electron trapping effects induced by oxygen. (*3*) The development of an air-stable ETOS that has a crystallographically engineered naphthalene tetracarboxylic diimide derivative has been reported recently. (*4*) Film deposition at a substrate

temperature of 70°C gave the best electron mobility (0.1 cm^2/Vs). However, uncontrolled deposition results in lowering the mobility to 10^{-3} cm^2/Vs. Precise control of substrate temperature is not always possible for devices with multi-layered structures because heating of the substrate may induce morphological changes in the underlying layers. Therefore, achieving high electron mobility in amorphous solid is one of the important challenges in the development of ETOS.

Electron transport in disordered amorphous molecular solids occurs via a hopping mechanism. This may be viewed as a one-electron reduction process of a neutral molecule concomitant with the oxidation of its anion. A large solid state electron affinity (Ea) is crucial in order to form a stable anion in the organic solid and reduce the trapping effects caused by oxygen. The attachment of strong electron withdrawing groups to extended π-electron conjugated systems is a well-established method for achieving a large Ea. Electron withdrawing groups such as nitro, (*5*) carbonyl, (*6*) and cyano (*7*) groups, or heterocyclic rings including metal complex of quinoline, (*8*) oxadiazole, (9) quinoxanline (*10*) have been reported. Unfortunately, the inclusion of strong electron withdrawing groups induces an energetic disorder and often leads to a decrease in hole (*11*) and electron (*12*) mobilities. This effect has been attributed to a dipolar disorder, which is essentially a fluctuation of energy in electron hopping sites, (*13*) and results in

highly dispersive electron transport. In this study, we report an ETOS with good air-stability and high electron mobility based on silole derivatives. Two unique electronic properties of the silole derivatives lead to a trap-free electron transport in the solid amorphous film. These are a large Ea originating from their σ^*-π^* conjugation and a high aromaticity of their anionic species.

2. Experimental details

Figure 1

The silole derivative shown in Fig.1 was synthesized by a one-step process from bis(phenylethynyl)silanes based on the intermolecular reductive cyclization followed by the palladium-catalyzed cross-coupling with aryl halide. (*14*) The crude products of 2,5-bis(6'-(2',2''-bipyridyl))-1,1-dimethyl-3,4-diphenylsilole (PyPySPyPy) was purified by recrystallization, column chromatography and vacuum sublimation. High purity tris (8-hydroxyquinolinolato) aluminum (III) (Alq_3) was purchased from H. W. Sands Corp. and used without further purification.

For the transport measurements, films were prepared on pre-patterned Indium Tin Oxide (ITO) coated glass substrates. The ITO substrates were cleaned by sonication in a de-ionized water bath, dried and exposed to UV/ozone at slightly elevated temperatures.

Subsequently, they were introduced into a glove box, where all the preparation steps took place in a dry nitrogen atmosphere with <1ppm oxygen and moisture concentrations. The organic films were deposited by vacuum sublimation at 10^{-6} mbar. The thickness of the organic films was in the range of 8–18 μm. The device preparation was finished by the deposition of a semitransparent aluminum (Al) layer which defined six devices per substrate each with an active area of 3 mm^2.

The mobilities were measured by the photoinduced time-of-flight technique (TOF). (*15*) Measurements were carried out in a custom-made vacuum container that was initially introduced into the glove box to load the samples in a dry nitrogen atmosphere. The influence of oxygen and moisture was evaluated by repeating measurements in air after overnight exposure of the sample to ambient atmosphere. A nitrogen laser with a nanosecond pulse width was used as the excitation source (λ=337nm), and was incident on the sample through the ITO electrode that was biased negative with respect to the Al electrode. The dark current was found to be negligible under this bias configuration indicating that ITO and Al act as non-injecting ("blocking") contacts for electron and hole injection, respectively. The electron mobility (μ_e) was determined from the conventional relationship: $\mu_e = L^2/(t_{TR} \cdot V)$, where t_{TR} is the transit time, L is the sample thickness and V is the applied voltage. For non-dispersive transients with well-defined plateaus, the mobility was determined from the time at which the photocurrent (I_{ph}) reached half of its plateau value ($t_{1/2}$ in Fig.2), while for dispersive transients, the transit time was determined from the inflection point (t_0) on a log(I_{ph})-log(t) plot. (*16*) All six devices on the same substrate were found to exhibit similar current-voltage characteristics and mobilities.

3. Results and discussion

Figure 2

A typical transient photocurrent for PyPySPyPy film (18μm) measured in a nitrogen atmosphere is shown in Fig. 2. The initial current spike is followed by a very clear and constant current plateau extending from 4 to 12 μs. The subsequent abrupt drop of the current is caused by the discharge of the electrons reaching the Al electrode. This is a "textbook" example of a TOF signal and clearly demonstrates nondispersive electron transport. The degree of carrier transport dispersion can be described by the tail broadening parameter W defined (*17*) as $W=(t_{1/2} - t_0)/ t_{1/2}$. For the transient photocurrent measured in nitrogen, we calculate W=0.22. To the best of our knowledge, this is the smallest W value ever reported for an ETOS and is comparable to that for hole transport in TPD which is known to be trap-free and non-dispersive. (*18*) The non-dispersive electron transport observed in this silole derivative suggests that electron trapping due to energetic disorder is very small or negligible. The measurement was repeated in air after overnight exposure to ambient atmosphere and no change was observed in the shape of the transient photocurrent. Indeed, we observe again W=0.22 even in air. Only a slight delay, less than 10%, in transit time was observed. These results suggest that oxygen does not

function as a significant trap in this silole. The decrease of photocurrent intensity observed in air is probably due to a decrease in the photocarrier generation efficiency. (*19*)

Figure 3

Figure 3 shows the electron mobilities of the films of PyPySPyPy and Alq_3 plotted as a function of the square root of the bias field. The electron mobility of the silole lies in the range from 9 x 10^{-5} cm^2/Vs to 2x10^{-4} cm^2/Vs. At any given electric field, the electron mobility of the silole derivative is more than two orders of magnitude higher than that of Alq_3. The Alq_3 film shows a highly dispersive transient photocurrent even in a nitrogen atmosphere, indicating the presence of intrinsic trap states. The highly dispersive transient photocurrent and the values of electron mobility of the Alq_3 films were consistent with those reported in the literature. (*8*) One of the origins of the electron traps in Alq_3 films can be attributed to the energetic disorder due to the large dipole moment of the Alq_3 molecule. The meridional and facial isomers of Alq_3 have μ=4.1 D and μ=7.1 D, respectively. (*20*) Conversely, the dipole moment of the PyPySPyPy is estimated to be 0.54 D based on the semi-empirical molecular orbital calculations. (*21*) Once air was introduced in the measurement cell, the transient photocurrent signal of the Alq_3 film became indiscernible and as such we were unable to determine its mobility. This is in clear contrast to what was observed for the silole derivative and suggests that oxygen acts

as a strong electron trap in the Alq_3 film. The presence of traps in an active layer is highly detrimental to current-driven devices such as OLEDs. Because, under dc operation, charge trapping will result in the built-up of space charge, which will increase operation voltage and degrade device performance.

Table 1

Table 1 lists the electron mobilities of selected amorphous molecular solid films prepared by vacuum vapor deposition on substrates held at room temperature. Bathophenanthroline seems to exhibit the highest electron mobility (*22*) among this group of molecules, twice as large as that of the silole derivative studied in this work. However, its transient photocurrent signal is highly dispersive suggesting the presence of intrinsic electron traps. In a sample that shows dispersive transport, the mobility is determined by t_0 that represents only the fastest portion of the carriers. As a result, the value of the mobility does not accurately reflect the electron transport properties of the vast majority of the carriers. NTDI shows a mobility (μ_e=1.0 x10^{-4} cm^2/Vs at 306 K) similar to that of the silole. However, the tail broadening parameter W=0.48 is almost twice as large as that of the silole derivative. Consequently, PyPySPyPy is the best amorphous material exhibiting nondispersive electron transport.

Two unique electronic properties of the silole ring may be responsible for the

nondispersive and high electron mobility of this material. First, the silole ring has a low-lying lowest unoccupied molecular orbital (LUMO) level due to the σ^*–π^* conjugation between a b1-symmetry σ^* orbital of the exocyclic silicon-carbon bond and a b1-symmetry π^* orbital of the carbons in the silole ring. (*23*) This brings about the high Ea of the silole ring without inducing electron traps due to energetic disorder. Second, the aromatic stabilization energy (ASE) of the silole anion is very large and indicates that the anion is thermodynamically favorable species. (*24*) In addition to the large ASE, diamagnetic susceptibility exaltations (DSE) found in the silole anion are extraordinarily negative and point to a large aromatic ring current. DSE is defined as the difference between the susceptibility measured for a compound and that calculated for the olefinic reference structure; hence, it is essentially the representation of the degree of electron delocalization. (*25*) The large ASE and DSE found in the silole anion may facilitate the reduction process on the silole ring concomitant with the electron hopping process. We thus propose that the air-stable and high electron mobility of the silole derivatives is realized because of the large Ea due to the σ^*–π^* conjugation and the extended delocalization of the negative charge on the silole ring.

Using the silole derivatives as an electron transport layer in OLEDs, a decrease of operation voltage has been reported. (*26*) This effect was attributed to the reduction of

electron injection barrier from the cathode to the silole layer due to its large Ea. However, the operation voltage does not depend only on the electron injection efficiency but also on the electron mobility. We have fabricated OLEDs using PyPySPyPy as an electron transporter and another silole derivative as an emitter and achieved external quantum efficiency of 4.8%. This efficiency was close to the theoretical limit (5%) for a fluorescent emitter with 100% photoluminescence quantum yield. Details of this study will be reported elsewhere.

Acknowledgements

We thank Dr. Gary Kushto (Naval Research Laboratory) for performing molecular orbital calculations of PyPySPyPy. Two of the authors (H. M. and Z. H. K.) gratefully acknowledge financial support from the Defense Advanced Research Projects Agency and the Office of Naval Research.

References

[1] J. H. Schön, S. Berg, Ch. Kloc, B.Batlog, Science, 287 (2000) 1022.

[2] J. H. Schön, Ch. Kloc, R. C. Haddon, B.Batlog, Science, 288 (2000) 656.

[3] R. C. Haddon, A. S. Perel, R. C. Morris, T. T. M. Palstra, A. F. Hebard, R. M. Fleming, Appl. Phys. Lett. 67 (1995) 121.

[4] H. E. Katz, A. J. Lovinger, J. Johnson, C. Kloc, T. Seigrist, W. Lim, Y.-Y. Lin, and A. Dodabalapur, Nature, 404 (2000) 478.

[5] W. D. Gill, J. Appl. Phys. 43 (1972) 5033.

[6] Y. Yamaguchi and M. Yokoyama, J. Appl. Phys. 70 (1991) 3726.

[7] N. C. Greenham, S. C. Moratti, D. D. C. Bradley, R. H. Friend, and A. B. Holmes, Nature 365 (1993) 628.

[8] R. G. Kepler, P. M. Beeson, S. J. Jacobs, R. A. Anderson, M. B. Sinclair, V, S. Valencia, and P. A. Cahill, Appl. Phys. Lett. 66 (1995) 3618.

[9] J. Bettenhausen, P. Strohriegl, W. Brutting, H. Tokuhisa, T. Tsutsui, J. Appl. Phys. 82 (1997) 4957.

[10] M. Redecker, D. D. C. Bradley, M. Jandke, P. Strrohriegl, Appl. Phys. Lett. 75 (1999) 109.

[11] R. H. Young, J. Phys. Chem. 99 (1995) 4230.

[12] P. M. Borsenberger, W. T. Grauenbrau, and E. h. Magin, Phys. Stat. Sol. B 190 (1995) 555.

[13] P. M. Borsenberger and H. Bässler, J. Chem. Phys., 95 (1991) 5327.

[14] S. Yamaguchi, T. Endo, M. Uchida, T. Izumizawa, K. Furukawa, K. Tamao, Chem. Eur. J. 6 (2000) 1683.

[15] A.R. Melnyk and D.M. Pai in: B.W. Rossiter and R.C. Baetzold (Eds.), Determination of electronic and optical properties, John Wiley & Sons, Inc. 1993.

[16] P.M. Borsenberger and D.S. Weiss, Organic Photoreceptors for Xerography, Marcel Dekker, New York, 1998, chap.7.

[17] L. B. Schein, Phil. Mag. B65 (1992) 795.

[18] H.-J. Yuh, M. Stolka, Phil. Mag. B58 (1988) 539.

[19] Y. Yamaguchi, M. Yokoyama, J. Appl. Phys. 70 (1991) 3726.

[20] A. Curioni, M. Boero, W. Andreoni, Chem. Phys. Lett. 294 (1998) 263.

[21] Values of the dipole moment for PyPySPyPy was calculated using the PM3 parameterization of the MNDO semiempirical method as is implemented in the Gaussian 98 system of programs. Gaussian 98, Revision A.6, Gaussian, Inc., Pittsburgh PA, 1998.

[22] S. Naka, H. Okada, H. Onnagawa, T. Tsutsui, Appl. Phys. Lett. 76 (2000) 197.

[23] S. Yamaguchi, K. Tamao, Bull. Chem, Soc, Jpn, 69 (1996) 2327.

[24] B.Goldfuss, P. von Rague, F. Hampel, Organometallics 15 (1996) 1755.

[25] H. J. Dauben, J. Am. Chem. Soc. 91 (1996) 1991.

[26] K. Tamao, M. Uchida, T. Izumizawa, K. Furukawa, S. Yamaguchi, J. Am. Chem. Soc., 118 (1996) 11974.

[27] H. Murata, M. Uchida, Z. H. Kafafi, To be published.

Figure 1 H. Murata et al.,

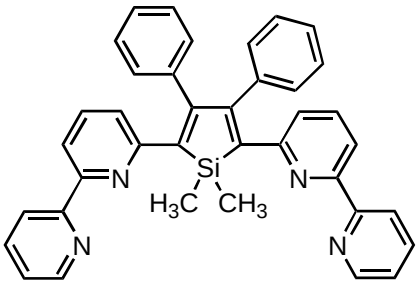

PyPySPyPy

Figure 2. H. Murata et al.

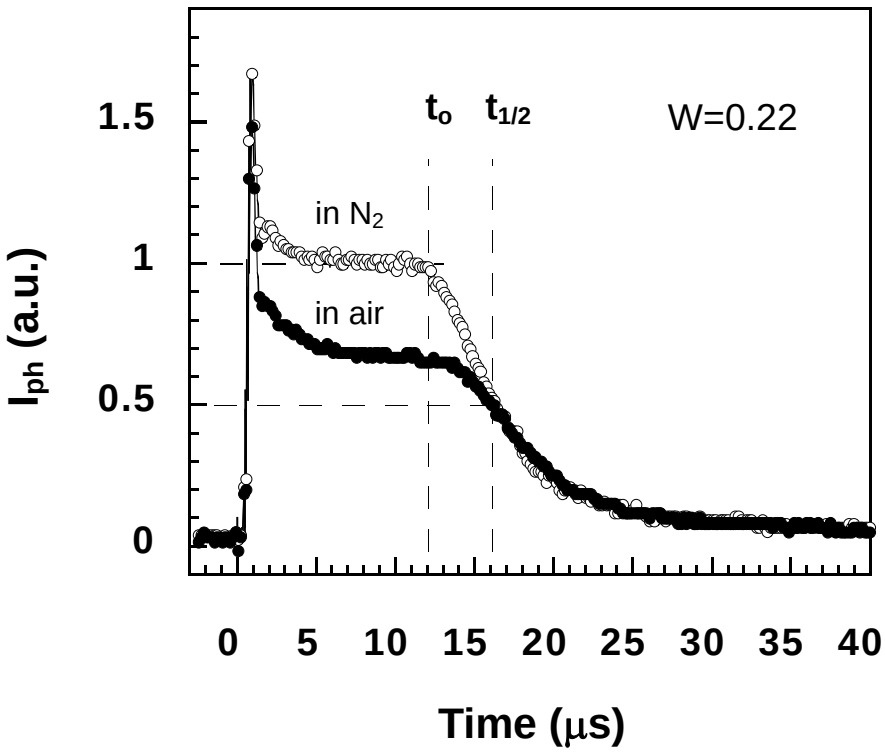

Figure 3. H. Murata et al.

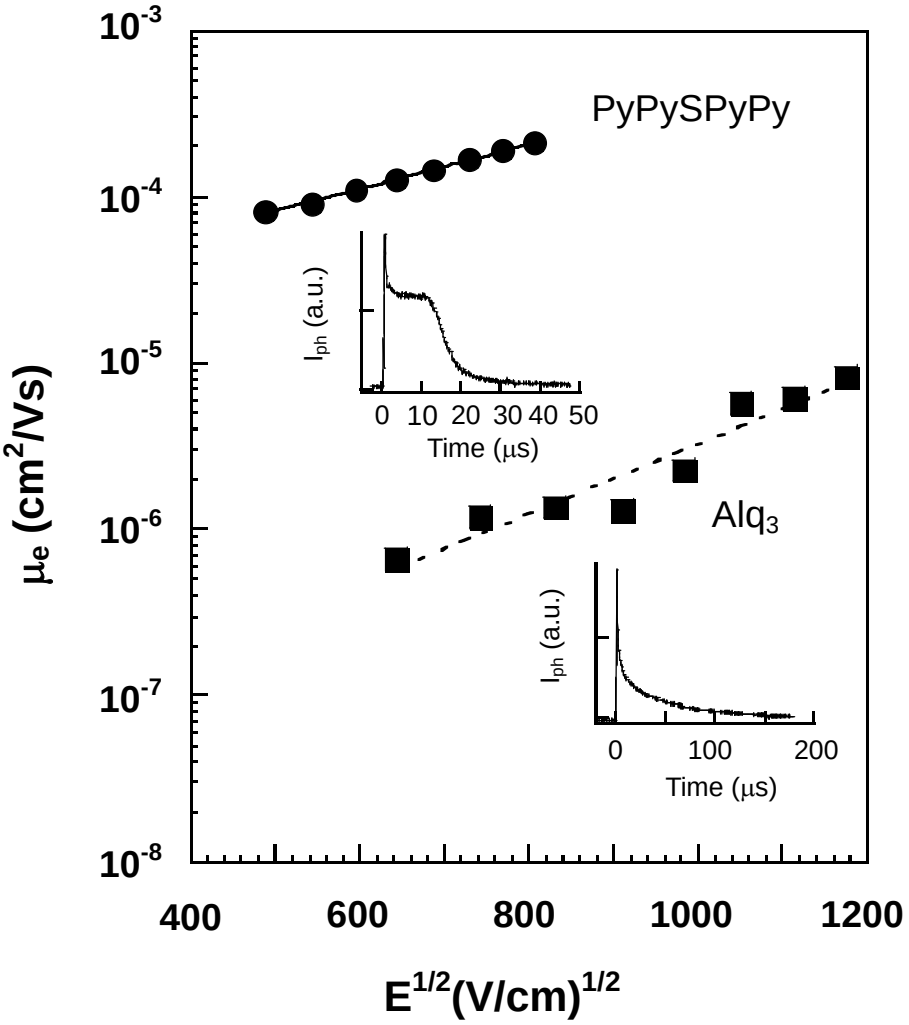

Table 1. H. Murata et al,

Table 1.

Electron mobilities of amorphous molecular solid films prepared by vacuum vapor deposition.

Material	μ_e* (cm^2/Vs)	Electric Field (V/cm)	Photocurrent signal‡	Atmo-sphere	Ref.
Alq_3	1.4×10^{-6}**	4.0×10^5	HD	N_2	8)
Alq_3	1.2×10^{-6}**	5.5×10^5	HD	N_2	This work
Bathophenanthroline	5.2×10^{-4}**	5.5×10^5	HD	N_2	22)
Starburst oxadiazole	1.2×10^{-6}**	7.0×10^5	D	-	9)
Starburst phenylquinoline	9.0×10^{-5}**	$\sim 1 \times 10^6$	D	-	10)
NTDI	1.0×10^{-4}†	5.0×10^5	ND (W=0.48)	air	12)
PyPySPyPy	2.0×10^{-4}†	6.4×10^5	ND (W=0.28)	air	This work

* Electron mobility measured by time-of-flight technique.

** Mobility was determined from the inflection point on a log (photocurrent)-log (time) plot.

† Mobility was determined from the time at which the current reached half of its plateau value ($t_{1/2}$).

‡ HD; highly dispersive, D; dispersive, ND; non-dispersive, $W = (t_{1/2} - t_0)/t_{1/2}$. (Ref. 16)

Figure Captions:

Figure1.

Chemical structure of 2,5-bis (6'-(2',2"-bipyridyl))-1,1-dimethyl-3,4-diphenyl silole (PyPySPyPy).

Figure 2.

Transient photocurrent signals (I_{ph}) for a PyPySPyPy film recorded at field E=0.55 MV/cm and at 300K. The film thickness was 18 μm. Measurements were performed in a nitrogen atmosphere and in air. The tail broadening parameter W was calculated using $W=(t_{1/2}-t_0)/t_{1/2}$, where t_0 is the time at the inflection point of the photocurrent and $t_{1/2}$ is the time it takes for the photocurrent to decay to half its value at t_0.

Figure 3.

The electron mobilities (μ_e) of films of PyPySPyPy and Alq_3 plotted as a function of the square root of the bias field. The insets show typical transient photocurrent signals for the films of PyPySPyPy (18 μm) and Alq_3 (8 μm), recorded at E=0.55MV/cm and E=1.1MV/cm, respectively.